A Contact-triggered Adaptive Soft Suction Cup

Tianqi Yue[1], Weiyong Si[2], Alix J. Partridge[3], Chenguang Yang[2], Andrew T. Conn[3], Hermes Bloomfield-Gadêlha[1] and Jonathan Rossiter[1]

***Abstract*— Suction adhesion is widely used by natural organisms for gripping irregular objects (e.g., rocks), but their artificial counterparts show less adaptation in the same situation. In addition, they can require complex sensing and control systems to function. In this paper, we present a contact-triggered suction cup with the ability to adapt to objects with complex and irregular shapes. The gripper has two states to adhere and release the object and the transformation from release to adhesion is passively triggered by the contact force, making it an autonomous gripper and removing the need for complex driven system. Once the suction cup experiences a contact force above a set threshold, it will automatically capture the contacting object. Only the resetting transformation from adhesion to release is actuated by a vacuum pump. The maximal suction force up to 15.1 N is generated on the non-flat surface with the suction cup diameter of 30 mm. The performance of this gripper is demonstrated on a 7 DoF robot arm which successfully picked up a variety of irregular objects. We believe that this contact-triggered gripper provides a new solution for low cost, energy-effective and adaptive soft gripping.**

I. Introduction

Suction-based grippers have been widely used in industry to carry glass plates, boxes and many other objects [1]. However, there is still a challenging issue - normal commercial suction cups, as well as some recently developed artificial ones, are only able to carry flat and smooth objects [2]–[8]. Some suction grippers can adhere to irregular objects by constantly pumping air out [1], [9]–[11], however, they did not address the leakage issue and induce side effects such as high energy consumption and annoying noise. Moreover, many suckers still need manual intervention to help the sucker attach and release. For example, reversing the pneumatic flow direction is the most widely used method to grip and release objects, but it needs at least one directional solenoid valve which adds complexity and cost. To improve the adaptation and automation, we develop a novel contact-triggered adaptive suction cup and demonstrate its functionality through a series of experiments. Fig.1 shows the proposed sucker mounted on a 7 DoF robot arm, having autonomously gripped and picked up a syringe. Additional three detailed snapshots show its adaptability.

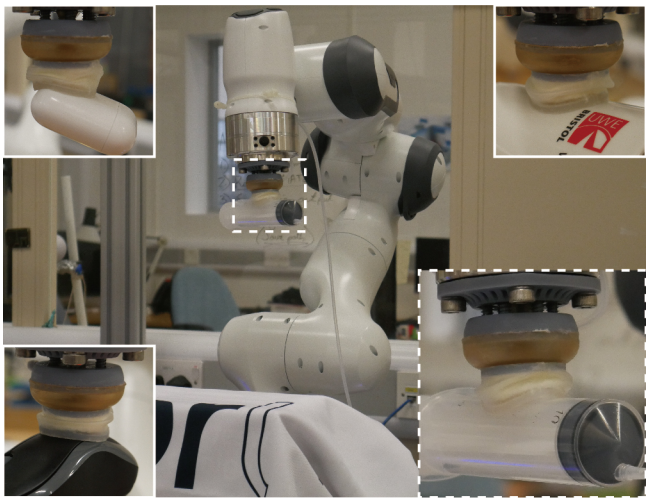

Fig. 1. The contact-triggered adaptive suction cup, carried by a robot arm and gripping a syringe. Three additional insert snapshots show its adaptation on an earphone case, a cup and a computer mouse.

Many researchers have made efforts to develop adaptive suction cups [9]–[17], and some exploit contact-triggering to improve automation [18], [19]. One challenge is to reduce the leakage which originates from gaps at the interface between the suction cup and the contact object. Proposals to solve this problem include granular jamming [9], [13], [14] and the use of a compliant bottom surface [16]–[18]. For example, Fujita et al. use robot hands to grip uneven surfaces by employing the granular jamming method [9]. Granular-jamming-based adaptive suckers still need pumping to resist leakage, therefore Tomokazu et al. combined granular jamming with multi-sucker array, realised better adaptation [14], [15]. Song et al. developed a self-sealing suction cup with compliant bottom layer to grip rough objects [16]. Tsukagoshi and Osada developed a hybrid suction cup by using both suction and stickiness, to help a drone attach to the ceiling [17].

Introducing passive triggering allows for a sucker with less requirement for visual servoing since adaptation and decision making are delegated to the automatic triggering of the sucker. Krahn et al. developed a soft-touch gripper that can automatically capture an object with little stimulus

[1]Tianqi Yue, Hermes Bloomfield-Gadêlha and Jonathan Rossiter are with the Department of Engineering Mathematics and Bristol Robotics Laboratory at the University of Bristol, Bristol, BS8 1TW, UK. {tianqi.yue, hermes.gadelha, jonathan.rossiter}@bristol.ac.uk

[2]Weiyong Si and Chenguang Yang are with the Faculty of Environment and Technology and Bristol Robotics Lab at the University of the West of England, Bristol, BS16 1QY, UK. Weiyong.Si@uwe.ac.uk, cyang@ieee.org

[3]Alix J. Partridge, Andrew T. Conn are with the Department of Mechanical Engineering and Bristol Robotics Laboratory at the University of Bristol, Bristol, BS8 1TR, UK. {alix.partridge, A.Conn}@bristol.ac.uk

TY is funded by Chinese Scholarship Council through award 201906120027. WS and CY were supported through EPSRC research grant EP/S001913. JR was supported through EPSRC research grants EP/T020792/1, EP/V026518/1, EP/S026096/1 and EP/R02961X/1, and by the Royal Academy of Engineering as a Chair in Emerging Technologies. AC was supported by EPSRC grants EP/T020792/1 and EP/R02961X/1.

but shows relatively low gripping force [18]. Jeong et al. designed an exoskeleton equipped with a multi-sucker system [19]. This sucker is also softly triggered to grip irregular objects. However, the adaptability is mainly achieved by the multi-sucker array, not individual sucker, and two directional solenoid valves are required.

In contrast to previous suckers, this work uses a novel method to improve adaptability and automation. In nature, the octopus generates adaptive negative copy on a variety of irregular objects by dexterously controlling the local movement of the muscles located on the rim of its suckers [20]–[22]. While the micro-sized sensors and musculature of the octopus are difficult to realise in artificial suckers, the proposed sucker mimics this behavior through passive adaptation. The proposed gripper can generate a negative copy of the contact surface by compressing a multi-layer structure, forming a soft, high-quality suction. A contact-triggering structure, which allows the sucker capture the object automatically, is also embeded in the proposed sucker, reduces the system complexity. In section II, we illustrate the concept, working principle and design method for realising the biomimetic functionality of the proposed suction gripper. In section III, we implement experiments to characterize the gripper's performance. In section IV, we carry out experiments using a 7 DoF robot arm to operate this gripper and demonstrate its practicability. Finally, conclusions are presented around some of its features, drawbacks and future developments.

II. Concept, Working Principle and Design

A. Contact-triggering and Shape-conformable Suction

The structure of this contact-triggered adaptive suction cup is shown in Fig.2. The gripper comprises two main parts: a triggering part and a suction part. The triggering part controls the transformation from inversion state to suction state, while the suction part is a multi-layer structure which plays the role of generating adaptive suction. The key part embeded in the triggering part is a rubber one-way duckbill valve which only allows air flow out. Initially, a vacuum pump connects to the air inlet and generates negative pressure differential (relative to atmospheric pressure) inside the actuation chamber. The negative pressure differential deforms the toroidal-shaped snap-through membrane into an inverted shape (Fig.3A). We call this process the 'resetting transformation', which is used for releasing the object and preparing for the next gripping. In the inversion state, the snap-through membrane pulls the periphery of the suction cup backward and simultaneously stores elastic energy. The inverted shape ensures the middle of the suction cup contacts the object first, thereby setting the gripper up for the strongest suction. When the contact force is exerted on the suction part, the suction part slides along the holes until an object (termed a plug here) push apart the leaflets of the valve (i.e., at threshold contact force), connects the inner chamber to atmosphere (as following Fig.4d shows). The stored elastic energy is released due to the pressure differential balance, which compresses the multi-layer structure and transitions the structure into the suction state. We term this step the 'suction transformation'. This trigger mechanism is inspired by [23] but invert their mechanism to control a negative rather than a positive pressure differential. The threshold at which the sucker transitions to suction state is defined by an array of six springs.

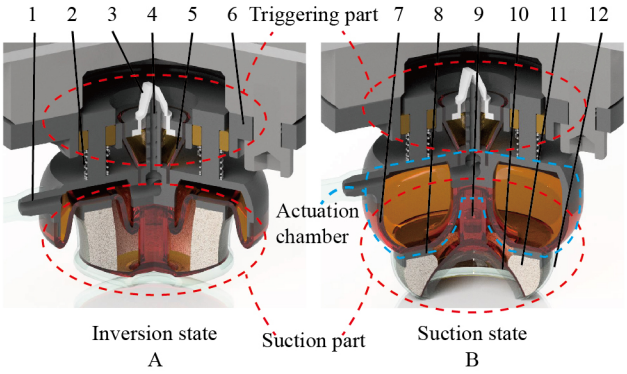

Fig. 2. Rendered image of the contact-triggered adaptive suction cup showing its concept. Note that no air flow exists at the moment shown in (A) and (B). (A) Inversion state: actuated by negative pressure differential, the snap-through membrane is inverted and pulls the periphery of the sucker into inverted shape. (B) Suction state: after being triggered, the multi-layer structure is compressed by the snap-through membrane. 1: air inlet. 2: circular array of six compression springs. 3: duckbill one-way soft valve. 4: plug. 5: sealing membrane. 6: flange. 7: toroidal-shaped membrane. 8: constraining plate. 9: polyurethane (PU) suction cup skeleton. 10: silicone pad. 11: porous latex ring. 12: silicone membrane.

The multi-layer structure of suction part consists of, from the top (furthest point from the object to be gripped) to the bottom, toroidal-shaped snap-through membrane, constraining plate, porous latex, suction cup skeleton and silicone pad. To explain its adaptive suction ability clearly, we cite the governing equation of leakage rate of suction cups presented by [24], which is given by

$$\dot{N} = K \cdot f\left(P_{\text{in}}\left(t\right)\right) \cdot \frac{L_y}{L_x} u_{\text{c}}^3\left(p\right)$$

where $\dot{N}$ is the number of gas molecules leaking into the suction region per unit time, K is the constant in related to the gas property, L_y and L_x are the length and width of contact sealing area, P_{in} is the inner pressure of the suction region, u_{c} is the surface separation termed the "critical junction" [24]. Based on Persson's contact and sealing theory [25], [26], u_{c} is negatively related to the contact pressure p sealing the suction cup and positively related to the suction bottom material modulus (assume the contact object is rigid). Therefore, reduction of L_y/L_x and increase of p are helpful for reducing leakage and improving suction quality.

By comparing normal Polyvinyl Chloride (PVC) suction cups (PPSC) (Fig.3A left) with the proposed sucker (Fig.3A right), we illustrate how this multi-layer structure helps to improve adaptive suction quality. Generally speaking, we want p to be high to reduce u_{c} (below 1 nm [24]) to slow the leakage. However, PPSC, including most previously designed suckers, cannot significantly increases p in terms

of a large range of surface topography. In other words, it is difficult for them to conform to the surface which is not only 'curved' in large scale (i.e., with large wavelength q), but also 'rough' in the small scale (with small q). The proposed sucker improves the adaptability in a wider range of q by the following logic. When it is pushed into an object, the porous latex conforms to surface shape in the large scale (similar to the property of honeycomb structure proposed in [27]) and exerts a compressive pressure on skeleton. The internal skeleton transfers compressive pressure to the silicone pad and generates an effective stretching force. Due to the higher contact pressure p and lower modulus than the normal PPSC, the silicone pad conforms to the micro-structures (roughness) and reduces u_c. Moreover, the width of contact region L_x of proposed sucker (Fig.3B right) is much larger than that of PPSC (Fig.3B left) since the compression of porous latex layer generates more evenly-distributed compressive force rather than the bending of PPSC. By this, the proposed sucker can reduce leakage rate $\dot{N}$ significantly and generate adaptive suction on a variety of irregular objects. Note that, we use a toroidal-shaped snap-through membrane, which has a defined central hub, to energy-effectively achieve this short-distance linear actuation. The toroidal membrane exhibits a similar snap-through behaviour to conventional cap-shaped membranes [28]–[31].

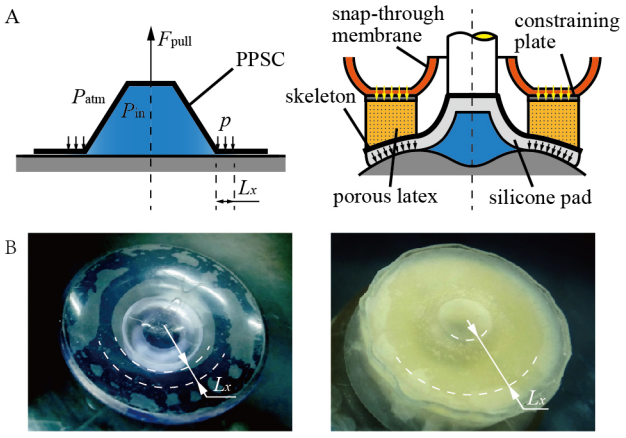

Fig. 3. Comparison between the normal PPSC and the proposed sucker. (A) Left: cross section diagram of the normal PPSC, adapted from [24]. Right: cross section diagram of proposed sucker. (B) Proposed sucker generates larger L_x than normal PPSC. Pictures are taken from the bottom view of the two suction cups adhering on a transparent PMMA plate.

The working principle of this gripper is as follows (shown in Fig.4): 1. initially, inner pressure is balanced with the atmosphere, the sucker is in its suction state and no object has been grasped (Fig.4a); 2. The vacuum pump pumps air out of the actuation chamber for 450 ms, then stops pumping. The suction cup then is in the inversion state and the pressure differential will remain negative without leakage because of the one-way valve (Fig.4b). Elastic energy is stored during the inversion state; 3. The robot arm moves the gripper towards an object until touching it (Fig.4c); 4. The robot continues to press the gripper onto the object. When the contact force exceeds the preset triggering threshold, the tip of the plug pushes open the soft duckbill valve and air begins to flow into the actuation chamber and the stored elastic energy of the snap-through membrane is released (Fig.4d). As the stored energy in the snap-through membrane is released, the multi-layer structure is compressed, thereby pushing the suction cup onto the object, generating shape conformation and a suction region; 5. Once a suction grip has been established, the robot arm lifts the object and the plug is pulled out of the duckbill valve by releasing the stored elastic potential energy of springs and the object gravity (Fig.4e); 6. Finally, after the gripping task has been completed, the vacuum pump operates to retract the periphery of the suction cup, breaking suction and releasing the object (Fig.4f).

B. Contact-trigger Mechanism Optimization

Trivially, the contact force F_c is given by $F_c = F_s + F_v$, where F_s is the total spring force and F_v is the resultant force exerted on the valve, which can be directly measured by experiments. The initial distance between the plug tip and the valve, d_i (see Fig.4), influences the minimal pushing displacement needed to open the valve (written as d_t, the threshold displacement) and the opening threshold force $F_v(d_t)$. Meanwhile, if the plug is too short (large d_i), it cannot push apart the leaflets of the valve to connect the actuation chamber with atmosphere; if the plug is too long (small d_i), it will remain between the leaflets thus stops the valve from being closed - that will hinder the sucker from being actuated next time and cause release failure. To optimize the structure and expand the functionality, we conduct experiments to understand how d_i influences d_t and $F_v(d_t)$. The spring force F_s is separately measured, so that the threshold contact force can be calculated by $F_c(d_t) = F_v(d_t) + F_s(d_t)$. The measured $F_v(d_t)$, $F_c(d_t)$, d_t are shown in Fig.5.

To measure F_v only, we remove the springs array in the system. Activating the vacuum pump (5 L/min) for 450 ms is sufficient to invert the snap-through membrane. The suction part is fixed on the base, and a linear stage moves the triggering part slowly to push the plug into the one-way duckbill valve until leakage is measured (the pressure differential sharply increases and a sudden decrease of contact force is observed) and the force at that instance is recorded. We tested d_i from 0 to 10 mm with interval 1 mm. As Fig.5 shows, when d_i is bigger than approximately 5 mm (R_2 region), the plug is too short to open the soft valve. When d_i is smaller than approximately 3 mm (R_1 region), the plug is too long, hindering the soft valve from being closed. $d_i \in \{3, 4, 5\}$ mm was found to be the region where the contact-trigger mechanism works well. As d_i increases within $\{3, 4, 5\}$ mm, the threshold contact force $F_c(d_t)$ also increases. The change of d_i does not influence $F_v(d_t)$ significantly, indicating that the increase of $F_c(d_t)$ is mainly contributed by the increase of spring force F_s. d_t also increases with d_i, indicating that the further the distance between the plug tip and valve, the longer the spring compression distance and hence the larger contact force needed to open the valve. To determine which d_i should to be used for our gripper design, we note that $d_i = 3$ mm

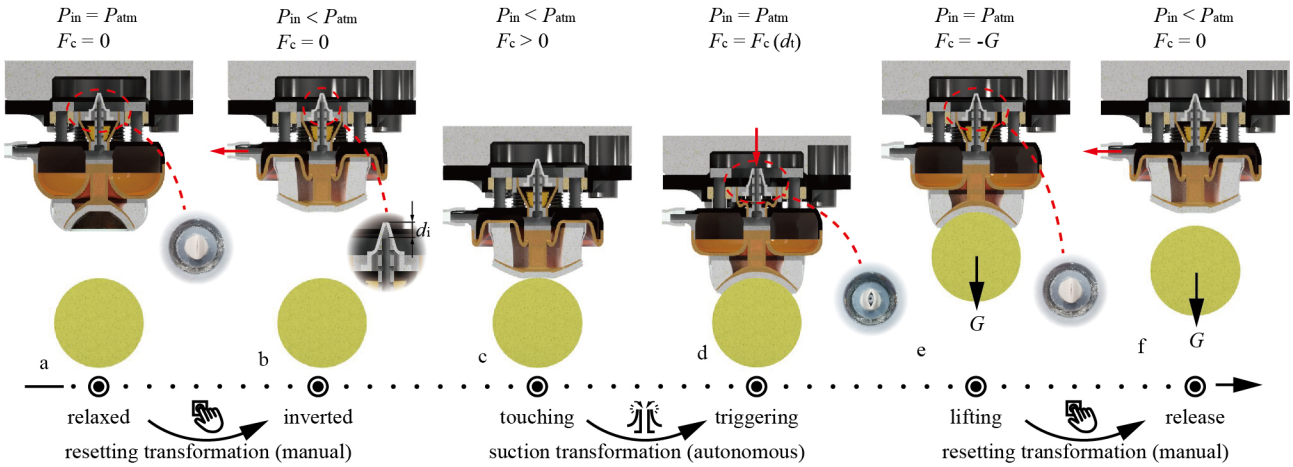

Fig. 4. A complete workflow for picking up an object and then releasing it. Red arrows indicate air flow direction. a: initial inner pressure is balanced with the atmosphere. b: vacuum pump works to place the gripper in the inversion state. c: the robot arm moves the gripper to touch an object. d: the contact force reaches the threshold value and the plug pushes open the soft one-way duckbill valve. The gripper transforms to the suction state. e: As the object is lifted, the plug retracts and the valve is closed again. f: the vacuum pump operates to release the object. P_{in}: inner pressure. P_{atm}: atmospheric pressure. F_c: contact force. $F_c(d_t)$: threshold contact force to open the valve. d_i: the initial distance between the plug and the soft valve.

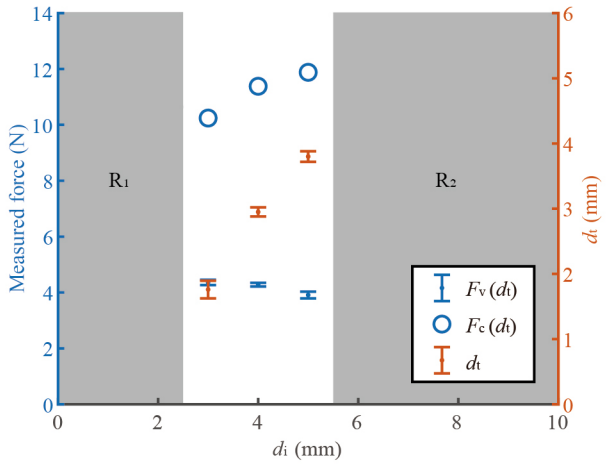

Fig. 5. Experimental data of $F_v(d_t)$, $F_c(d_t)$ and d_i. R_1: region where the soft valve cannot be closed since the plug is too long. R_2: region where the soft valve cannot be opened since the plug is too short. The measured spring constant of each single compression spring is 0.17 N/mm.

yields the smallest triggering force ($F_c(d_t) = 10.24$ N) and requires the smallest displacement d_t to open the valve.

C. Fabrication of the gripper and samples

According to Fig.2, all the grey parts, including the lid, flange, plug and constraining plate are 3D printed (Anycubic Photon Mono X, Anycubic, China). All the amber parts, including the toroidal-shaped snap-through membrane, the suction cup skeleton and the sealing membrane, are cast from PU rubber (PT Flex 60, Polytek Development Corp, United States). Silicone pad is cast from Ecoflex 00-50^{TM} (Smooth-On Inc., United States). Liquid rubbers and silicone are degassed before casting, and baked for 1 hour at 40 °C for curing. The thickness of snap-through membrane and silicone pad influence the sucker performance a lot. Thicker the snap-through membrane, more the membrane compresses porous latex and quicker the transition from inversion to suction state, but needs higher pressure differential to invert. Thicker the skeleton and silicone pad, better for sucker to conform to micro-structure, but will be more difficult to be bent to conform to surface shape. To optimize, we found the toroidal-shaped snap-through membrane, the suction cup skeleton and the silicone pad with thicknesses of 1.5, 0.5 and 2.5 mm, respectively, give a good final performance across a wide range of objects. The sealing membrane is with 0.75 mm thickness. The hollow-cylinder-shaped porous latex is cut from a synthetic porous latex sheet to dimension of 18.5×30.5×25 mm (inner diameter×outer diameter×thickness). The duckbill one-way valve (Standard Elastomeric Valve Components, Minivalve) can withstand up to 3 bar reverse pressure differential [23]. The peripheral silicone membrane is 0.5 mm thick and has shore 60A hardness. The six compression springs have dimensions 5×0.3×10 mm (outer diameter×wire diameter×free length). Sil-Poxy^{TM} (Smooth-On Inc., United States) is used for assembling soft parts to ensure flexibility, while Loctite Precision is used to assemble rigid parts. Before assembling, the springs are pre-compressed by 5 mm.

The quadric samples used in the following experiments are made by resin, which is also 3D printed. After printing, contact surfaces are polished using fine sandpaper (5000 grit).

III. Suction Performance Characterization

The performance of this gripper is evaluated from two aspects: i) the practical threshold contact force and the successful triggering rate, and ii) the adaptive suction performance. The experimental setup for testing is shown in Fig.6, and the evaluation process is implemented as follows. First,

the vacuum pump works for 450 ms to invert the suction cup. Second, the linear stage moves downward for a specific distance to let the gripper contact the specimen (fixed to the load cell) and trigger the valve. Third, the linear stage begins to move upward, until the suction cup breaks off from the specimen. The real-time contact force and the pressure differential throughout the experimental process are recorded by a load cell (SB, jl-maxwell, China) and a pressure sensor (bmp280, Bosch, Germany), respectively. Note that, the load cell in this experiment setup and the following on-robot setup is not needed in practical application. It is used to measure the threshold force to compare with the theoretical value.

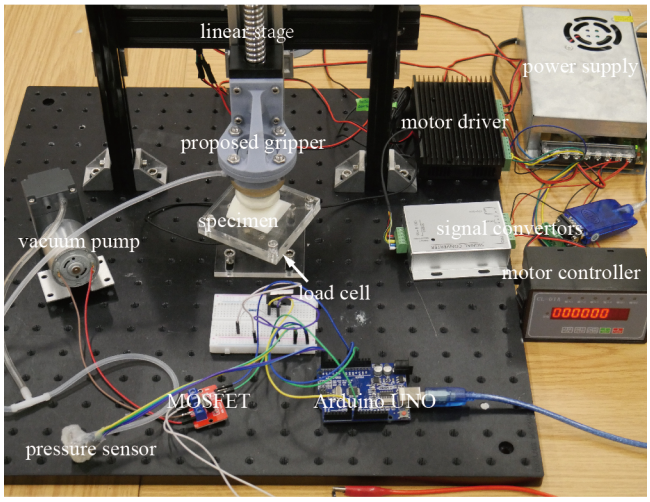

Fig. 6. The experimental setup for characterizing the gripper's functionality. The linear stage is controlled by the motor controller and driver, the vacuum pump and pressure sensor are controlled by an Arduino UNO board. Once the push button on the breadboard is pressed, the pump will work for 450 ms. Force signals and pressure differential signals are read through two separate serial communication lines on the PC.

The contact-trigger process can be clearly observed from the real-time contact force and pressure differential shown in Fig.7, and maximum suction forces can be recorded. When the vacuum pump begins to work (P_1), the pressure differential decreases to -12 kPa remains around -10 kPa. The linear stage moves downward and the sucker contacts the specimen (P_2). When the contact force F_c reaches its threshold ($F_c(d_t)$), the soft valve is opened by the plug and the pressure differential decreases sharply to atmospheric pressure. The threshold point is quite clear at 8.8 s. An additional compressive force exerts on the sample after triggering, since the snap-through membrane begins to recover thereby compresses the porous latex. As the object is then lifted, the contact force begins to decrease. In this process, the contact force fluctuates slightly as the snap-through membrane is recovering its shape as the gripper is being lifted. This snap-through momentarily exerts extra contact force to the object (see Supplementary Video S1). Finally, the suction cup breaks off from the specimen and the maximal suction force F_{s_max} is recorded at the breaking instance (P_3).

A series of quadric-surface specimens are used for characterizing the sucker adaptive suction performance. We used

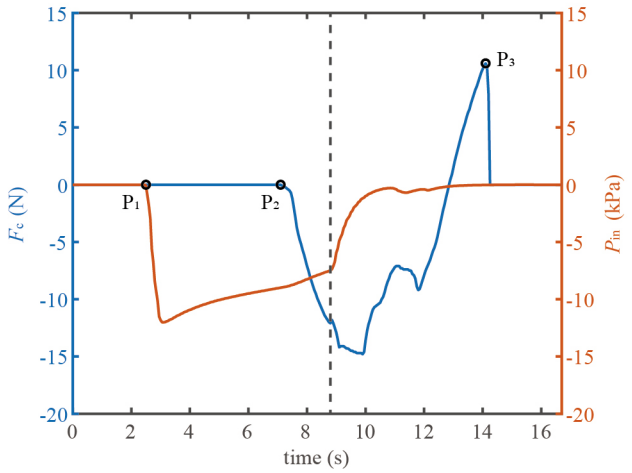

Fig. 7. The contact force and pressure differential recorded during suction and break-off tests on a non-flat surface. P_1: the vacuum pump begins evacuate the inner chamber. P_2: contact begins. P_3: the instance of break-off (sucker releases from object). Dashed line: the triggering instance.

ellipsoids (EPs), hyperbolic paraboloids (HPs) and parabolic cylinders (PCs). These 3D surface profiles are extremely challenging for suckers with limited adaptability. The equations determining the surface of the EPs, HPs and PCs are written as $x^2/a^2+y^2/b^2+z^2/c^2=1$, $x^2/a^2-y^2/b^2+z=0$ and $x^2+2az=0$, respectively. Here, we set $a=0.5b=c$ and then set $a=25,20,15$ for EPs and PCs, set $a=8,7,6$ for HPs, to increase the curvature of the samples at a regular interval. We conducted the suction and break-off tests described above for all samples for ten times. The experimental results are shown in Fig.8. Supplementary Video S1 shows the experimental procedures in details.

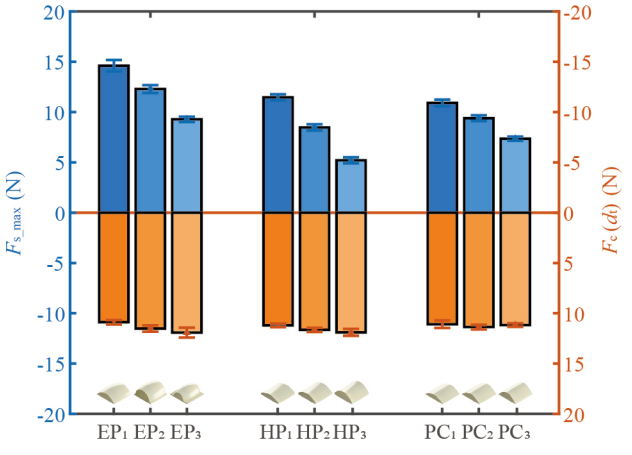

Fig. 8. Experimental results showing suction gripping performance on quadric surfaces. Objects with subscripts 1, 2 and 3 correspond to shape parameter $a=25$, 20, 15 (EPs and PCs) and $a=8$, 7, 6 (HPs), respectively. For clarity, we reverse the right hand y axis ($F_c(d_t)$).

The gripper is successfully triggered in every test. Fig.8 shows that the gripper can generate considerable suction force on complex surfaces, up to 15.1 N on the EP_1 surface.

The maximum suction force reduces with increased surface curvature, falling to 9.28 N, 5.20 N and 7.35 N on EP_3, HP_3 and PC_3, respectively. In all cases the suction cup was able to automatically establish a strong and leak-free suction. The experimental results indicate the potential of the suction gripper to pick up real-world objects with a large range of curvatures and irregularity. The measured threshold contact force $F_c(d_t)$ is stable on different surfaces, with average measured $F_c(d_t) = 11.41$ N. This value, as discussed later, can be readily reduced. This value is larger than the previous measured value (10.24 N in Fig.5). That might be caused by the frictional force which was neglected. However, this will not influence the gripper's application significantly.

We further measured the maximal curvature of the object that the proposed sucker can grip by testing spheres made by POM (Polyoxymethylene) with diameter in the range of 10 mm to 20 mm. Since the spheres have different masses, we define a successful grip as one where the sucker can pick up the sphere and hold it for one minute. Each sphere is tested ten times and the experimental results are shown in Fig.9, with video shown in Supplementary Video S1. The maximal curvature ensuring successful gripping is given by the sphere with diameter of 13 mm.

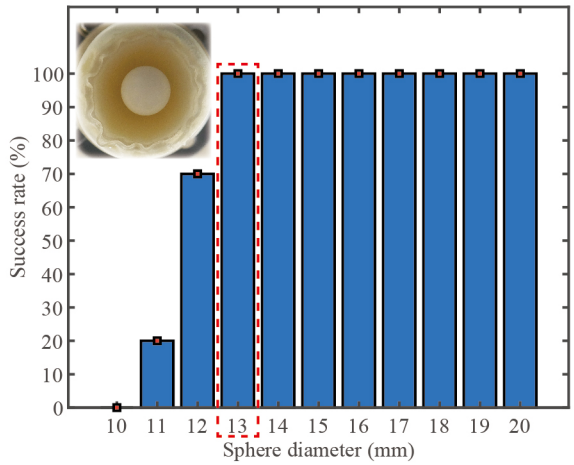

Fig. 9. The gripping success rate on spheres with different curvature. The proposed sucker delivers 100% success rate on spheres with diameter $\geq$ 13 mm, and this falls to 0% success rate on spheres with diameter $\leq$ 10 mm. The insert shows the situation when the proposed sucker is gripping a sphere with diameter of 13 mm.

IV. Gripping Real-world Objects: On-robot Test

The performance of the proposed sucker is evaluated through a series of on-robot experiments using a Franka Emika 7-DoF robot arm. Grasping tasks undertaken by rigid robotic arms often require state-of-the-art compliant control approaches, e.g., hybrid force-position control [32], impedance control [33], and admittance control [34]. However, it is still challenging for the robot arm to execute the contact and manipulation tasks, especially when controlling the transition process from free motion to the contact state. In our experiments, we replace the rigid gripper of the robot arm with the proposed sucker and demonstrate its ability to automatically grasp various objects, including textured and curved surfaces. By integrating the proposed soft gripper and compliant control methods, the robot can safely and reliably grasp irregular objects. The softness of the gripper not only improves compliance and adaptability, but also safety. In the first part of this section, we use the robot to consecutively grip then release three objects. Fig.10 shows the whole process of the experiments.

The snapshots in Fig.10 shows a series of consecutive tasks to grip then release objects. The vacuum pump, controlled by an Arduino board, works for 450 ms when a push button is pressed, which is manually controlled. It is possible to integrate the controller of the robot and the vacuum pump into one system in the future. Note that the force measured at the start point is non-zero because of the weight of the gripper and some connectors. Also, since the force is calculated through joint torque sensors in the robot arm, the relative force accuracy is 0.8 N, but this is sufficient for the experiment. In terms of the control of the rigid arm, we adopted a composite control strategy consisting of impedance controller and hybrid force-position controller. In the free motion stage (yellow regions), the impedance controller is used to control the position, and the hybrid force-position controller is used to adjust the control force when the suction cup contacts with the objects (green regions).

The robot arm equipped with the soft gripper is also used to grasp 9 different objects automatically to show its adaptability and practicability, as shown in Fig.11. Three bottles with different curvatures, a roll of tape, a cone-shaped cup, a syringe, a computer mouse, an orange and an earphone case are readily and safely grasped.

Fig.11 demonstrates that the developed autonomous suction cup gripper is able to grasp a wide range of objects. The grasping success rate is high (around 90%). Note that we placed the object by hand on a flat surface and did not orient them for best (perpendicular) gripping. In practice, a more sophisticated control system, for example using machine vision to determine object orientation, could be used to further increase this success rate. Supplementary Video S2 shows the picking and releasing of these objects.

V. Conclusions

In this paper, we proposed a novel contact-triggered adaptive suction cup. Based on the experimental results, the gripper can generate suction forces up to 15.1 N on non-flat surfaces. When the contact force exceeds a preset contact force, the gripper is automatically triggered by its mechanical-feedback structure to generate a powerful suction region. The sucker can be actuated by a low pressure differential (~ -12 kPa), and the trigger mechanism removes the need to change air flow direction, thereby reducing the system complexity and cost. Using a 7 DoF robot arm, the adaptability of the suction cup and the effectiveness of the contact-trigger mechanism were demonstrated through experiments gripping and lifting irregular objects.

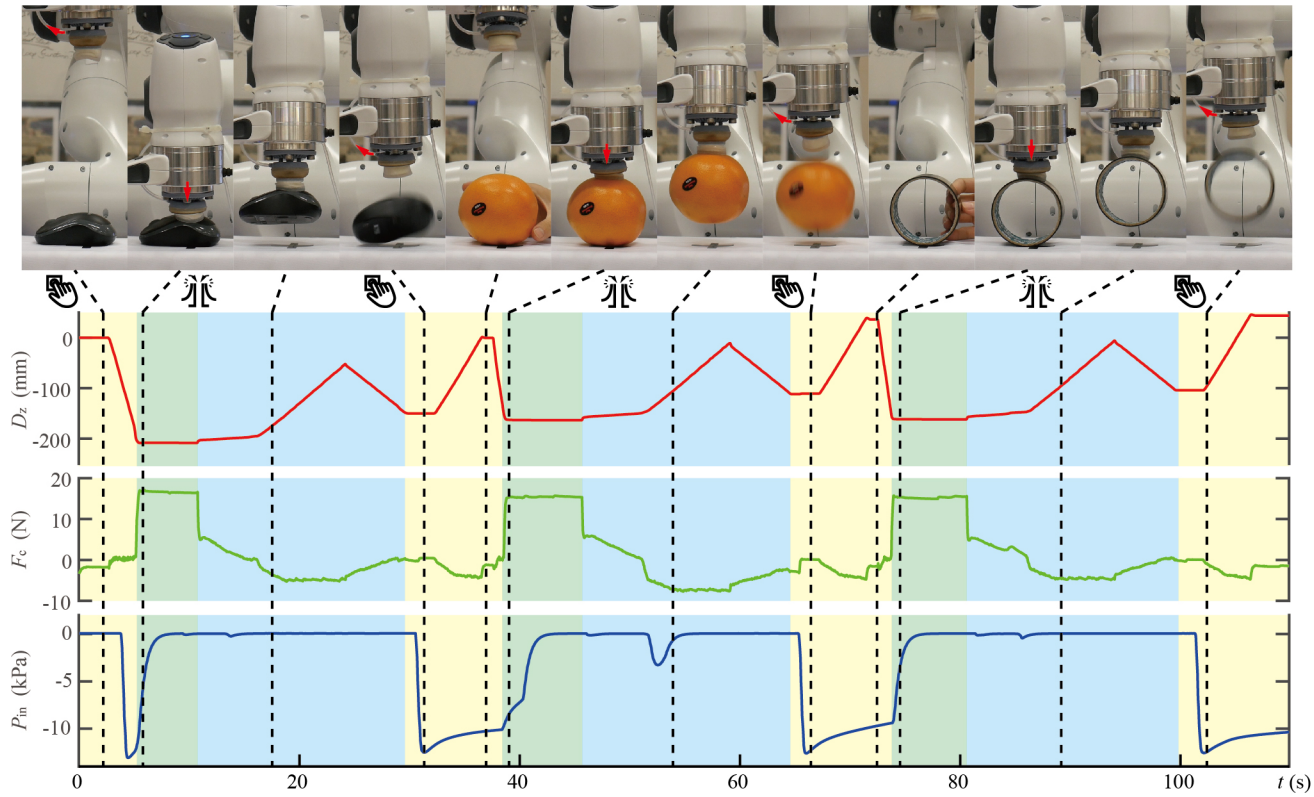

Fig. 10. Experiments for consecutively gripping three objects: a computer mouse, an orange and a roll of tape. Every cycle is divided into three parts. Red arrows indicate air flow direction. Yellow regions: release the previous object and prepare for gripping the next one, controlled by the robot impedance controller. Green regions: automatic suction, and slow lifting of the object, controlled by the hybrid force-position controller. Blue region: lift the object for a period to verify the longevity of the suction before releasing.

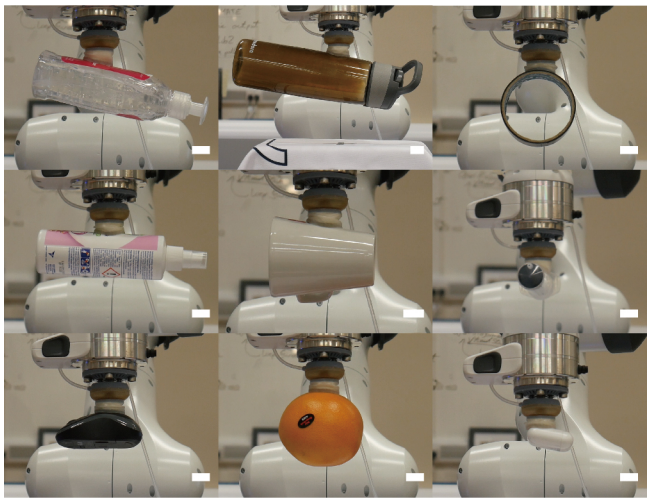

Fig. 11. Grasping nine different irregular objects. The surface shape of tested objects includes cylinders with different curvature, a cone, a sphere with texture and curved irregular shape. Scale bars: 20 mm.

To show the advances of the proposed sucker, we compare performance with recently developed adaptive suckers in Tab.I. This shows that the proposed sucker can generate a relatively higher suction force with smaller size. All adaptive suckers in Tab.I have their unique features, such as liquid-enhanced suction [14], soft-touch gripping [19], [35], adaption to edged shape [11] or rough surface [16], and stickiness [17].

TABLE I

COMPARISON BETWEEN SOFT ADAPTIVE SUCTION GRIPPERS

Gripper	d **(mm)**	F_{s_max} **(N)**	**Ref.**
soft-touch-triggered sucker	60	12	[35]
origami sucker	41	5.2	[11]
jamming sucker	60	46	[14]
self-sealing sucker	18	7.7	[16]
soft-touch on-glove sucker	14	3.19	[19]
sticking sucker	55	80	[17]
This work	30	15.1	-

This gripper obtains its adaptive suction ability by compressing a multi-layer soft structure, generating shape conformation to the contact surface. Its contact-trigger mechanism is realised by pushing open a duckbill soft one-way valve. This gripper is easy to fabricate and is low cost, and requires little external input beyond a very small vacuum pump to reset the suction cup. This force threshold is determined by the stiffness of the springs that separate the suction part from the triggering part (Fig.2). Up to 15.1 N suction force can be generated on a non-flat surface with a suction region diameter of 30 mm and the gripper shows high adaptability, autonomy and low energy consumption. Limits of this sucker could be: 1. Relatively slow response time, i.e., the transition to full suction. That is due to the recovery force at the instance

of triggering being only slightly less than the force needed to compress the porous latex. 2. Failure on objects that are not well-centered. That could be addressed by introducing a gimbal [19] or sensors [36] to the proposed sucker. 3. Limit on gripping delicate objects, because of the relatively high triggering force [18], [19] in this embodiment. However, by using softer springs and/or a different valve design (such as a small poppet valve) the contact force can be significantly reduced. Future work will focus on shortening the response time by optimizing the sucker geometry, introducing sensor to make the sucker more "morphologically intelligent". We believe the proposed sucker will enable more effective, lower cost and energy efficient object manipulation in applications including human-robot interaction, object picking and safe healthcare robotics.

REFERENCES

[1] Piab, "Suction cups for industry," https://www.piab.com/suction-cups-and-soft-grippers/ Accessed July 9, 2021.

[2] S. Sareh, K. Althoefer, M. Li, Y. Noh, F. Tramacere, P. Sareh, B. Mazzolai, and M. Kovac, "Anchoring like octopus: biologically inspired soft artificial sucker," *Journal of the royal society interface*, vol. 14, no. 135, p. 20170395, 2017.

[3] F. Tramacere, L. Beccai, F. Mattioli, E. Sinibaldi, and B. Mazzolai, "Artificial adhesion mechanisms inspired by octopus suckers," in *2012 IEEE International Conference on Robotics and Automation*. IEEE, 2012, pp. 3846–3851.

[4] H. Bing-Shan, W. Li-Wen, F. Zhuang, and Z. Yan-zheng, "Bio-inspired miniature suction cups actuated by shape memory alloy," *International Journal of Advanced Robotic Systems*, vol. 6, no. 3, p. 29, 2009.

[5] N. Sholl, A. Moss, W. M. Kier, and K. Mohseni, "A soft end effector inspired by cephalopod suckers and augmented by a dielectric elastomer actuator," *Soft robotics*, vol. 6, no. 3, pp. 356–367, 2019.

[6] F. Tramacere, M. Follador, N. Pugno, and B. Mazzolai, "Octopus-like suction cups: from natural to artificial solutions," *Bioinspiration & biomimetics*, vol. 10, no. 3, p. 035004, 2015.

[7] H. Kumamoto, N. Shirakura, J. Takamatsu, and T. Ogasawara, "Underwater suction gripper for object manipulation with an underwater robot," in *2021 IEEE International Conference on Mechatronics (ICM)*. IEEE, 2021, pp. 1–7.

[8] S. Wang, L. Li, W. Sun, D. Wainwright, H. Wang, W. Zhao, B. Chen, Y. Chen, and L. Wen, "Detachment of the remora suckerfish disc: kinematics and a bio-inspired robotic model," *Bioinspiration & Biomimetics*, vol. 15, no. 5, p. 056018, 2020.

[9] M. Fujita, S. Ikeda, T. Fujimoto, T. Shimizu, S. Ikemoto, and T. Miyamoto, "Development of universal vacuum gripper for wall-climbing robot," *Advanced Robotics*, vol. 32, no. 6, pp. 283–296, 2018.

[10] K. Gilday, J. Lilley, and F. Iida, "Suction cup based on particle jamming and its performance comparison in various fruit handling tasks," in *2020 IEEE/ASME International Conference on Advanced Intelligent Mechatronics (AIM)*. IEEE, 2020, pp. 607–612.

[11] Z. Zhakypov, F. Heremans, A. Billard, and J. Paik, "An origami-inspired reconfigurable suction gripper for picking objects with variable shape and size," *IEEE Robotics and Automation Letters*, vol. 3, no. 4, pp. 2894–2901, 2018.

[12] J. Shintake, V. Cacucciolo, D. Floreano, and H. Shea, "Soft robotic grippers," *Advanced Materials*, vol. 30, no. 29, p. 1707035, 2018.

[13] J. R. Amend, E. Brown, N. Rodenberg, H. M. Jaeger, and H. Lipson, "A positive pressure universal gripper based on the jamming of granular material," *IEEE transactions on robotics*, vol. 28, no. 2, pp. 341–350, 2012.

[14] T. Tomokazu, S. Kikuchi, M. Suzuki, and S. Aoyagi, "Vacuum gripper imitated octopus sucker-effect of liquid membrane for absorption," in *2015 IEEE/RSJ International Conference on Intelligent Robots and Systems (IROS)*. IEEE, 2015, pp. 2929–2936.

[15] T. Takahashi, M. Suzuki, and S. Aoyagi, "Octopus bioinspired vacuum gripper with micro bumps," in *2016 IEEE 11th Annual International Conference on Nano/Micro Engineered and Molecular Systems (NEMS)*. IEEE, 2016, pp. 508–511.

[16] S. Song, D.-M. Drotlef, D. Son, A. Koivikko, and M. Sitti, "Adaptive self-sealing suction-based soft robotic gripper," *Advanced Science*, p. 2100641, 2021.

[17] H. Tsukagoshi and Y. Osada, "Soft hybrid suction cup capable of sticking to various objects and environments," in *Actuators*, vol. 10, no. 3. Multidisciplinary Digital Publishing Institute, 2021, p. 50.

[18] J. M. Krahn, F. Fabbro, and C. Menon, "A soft-touch gripper for grasping delicate objects," *IEEE/ASME Transactions on Mechatronics*, vol. 22, no. 3, pp. 1276–1286, 2017.

[19] S. Jeong, P. Tran, and J. P. Desai, "Integration of self-sealing suction cups on the flexotendon glove-ii robotic exoskeleton system," *IEEE Robotics and Automation Letters*, vol. 5, no. 2, pp. 867–874, 2020.

[20] P. Graziadei, "Receptors in the suckers of octopus," *Nature*, vol. 195, no. 4836, pp. 57–59, 1962.

[21] W. M. Kier and A. M. Smith, "The structure and adhesive mechanism of octopus suckers," *Integrative and Comparative Biology*, vol. 42, no. 6, pp. 1146–1153, 2002.

[22] W. M. Kier and A. M. Smith, "The morphology and mechanics of octopus suckers," *The Biological Bulletin*, vol. 178, no. 2, pp. 126–136, 1990.

[23] A. J. Partridge and A. T. Conn, "Passive, reflex response units for reactive soft robotic systems," *IEEE Robotics and Automation Letters*, vol. 5, no. 3, pp. 4014–4020, 2020.

[24] A. Tiwari and B. Persson, "Physics of suction cups," *Soft matter*, vol. 15, no. 46, pp. 9482–9499, 2019.

[25] C. Yang and B. Persson, "Contact mechanics: contact area and interfacial separation from small contact to full contact," *Journal of Physics: Condensed Matter*, vol. 20, no. 21, p. 215214, 2008.

[26] B. Lorenz, N. Rodriguez, P. Mangiagalli, and B. Persson, "Role of hydrophobicity on interfacial fluid flow: Theory and some applications," *The European Physical Journal E*, vol. 37, no. 6, pp. 1–14, 2014.

[27] J. Lee, Y.-S. Seo, C. Park, J.-s. Koh, U. Kim, J. Park, H. Rodrigue, B. Kim, and S.-H. Song, "Shape-adaptive universal soft parallel gripper for delicate grasping using a stiffness-variable composite structure," *IEEE Transactions on Industrial Electronics*, 2020.

[28] A. Pandey, D. E. Moulton, D. Vella, and D. P. Holmes, "Dynamics of snapping beams and jumping poppers," *EPL (Europhysics Letters)*, vol. 105, no. 2, p. 24001, 2014.

[29] P. Rothemund, A. Ainla, L. Belding, D. J. Preston, S. Kurihara, Z. Suo, and G. M. Whitesides, "A soft, bistable valve for autonomous control of soft actuators," *Science Robotics*, vol. 3, no. 16, 2018.

[30] D. J. Preston, P. Rothemund, H. J. Jiang, M. P. Nemitz, J. Rawson, Z. Suo, and G. M. Whitesides, "Digital logic for soft devices," *Proceedings of the National Academy of Sciences*, vol. 116, no. 16, pp. 7750–7759, 2019.

[31] D. J. Preston, H. J. Jiang, V. Sanchez, P. Rothemund, J. Rawson, M. P. Nemitz, W.-K. Lee, Z. Suo, C. J. Walsh, and G. M. Whitesides, "A soft ring oscillator," *Science Robotics*, vol. 4, no. 31, 2019.

[32] A. G. Marin and R. Weitschat, "Unified impedance and hybrid force-position controller with kinestatic filtering," in *2016 IEEE/RSJ International Conference on Intelligent Robots and Systems (IROS)*. IEEE, 2016, pp. 3353–3359.

[33] C. Yang, G. Ganesh, S. Haddadin, S. Parusel, A. Albu-Schaeffer, and E. Burdet, "Human-like adaptation of force and impedance in stable and unstable interactions," *IEEE transactions on robotics*, vol. 27, no. 5, pp. 918–930, 2011.

[34] G. Peng, C. P. Chen, and C. Yang, "Neural networks enhanced optimal admittance control of robot-environment interaction using reinforcement learning," *IEEE Transactions on Neural Networks and Learning Systems*, 2021.

[35] J. M. Krahn, F. Fabbro, and C. Menon, "A soft-touch gripper for grasping delicate objects," *IEEE/ASME Transactions on Mechatronics*, vol. 22, no. 3, pp. 1276–1286, 2017.

[36] H. J. Lee, S. Baik, G. W. Hwang, J. H. Song, D. W. Kim, B.-y. Park, H. Min, J. K. Kim, J.-s. Koh, T.-H. Yang, *et al.*, "An electronically perceptive bioinspired soft wet-adhesion actuator with carbon nanotube-based strain sensors," *ACS nano*, vol. 15, no. 9, pp. 14 137–14 148, 2021.